Supporting Information for "All-Optical Chirality-Sensitive Sorting *via* Reversible Lateral Forces in Interference Fields"

Tianhang Zhang, Mahdy Rahman Chowdhury Mahdy, Yongmin Liu, Jing Hua Teng, Chwee Teck Lim，Zheng Wang, and Cheng-Wei Qiu

1. Derivation of optical force a chiral dipole

We start from the equation (1) and (9) in the main text to calculate the optical force on a chiral dipole

$$\begin{aligned} \boldsymbol{p} &= \alpha_e \boldsymbol{E} + i\chi \boldsymbol{H} \\ \boldsymbol{m} &= -i\chi \boldsymbol{E} + \alpha_m \boldsymbol{H} \end{aligned} \tag{S1}$$

$$\left\langle \boldsymbol{F} \right\rangle = \frac{1}{2}\mathrm{Re}[\boldsymbol{p}(\nabla \otimes \boldsymbol{E}^*) + \boldsymbol{m}(\nabla \otimes \boldsymbol{H}^*) - \frac{ck^4}{6\pi}\frac{1}{\sqrt{\varepsilon_b \mu_b}}(\boldsymbol{p} \times \boldsymbol{m}^*)] \tag{S2}$$

The first two terms in (S2) can be written as:

$$\begin{aligned} \left\langle \boldsymbol{F}_{EM} \right\rangle &= \frac{1}{2}\mathrm{Re}[(\alpha_e \boldsymbol{E} + i\chi \boldsymbol{H})(\nabla \otimes \boldsymbol{E}^*) + (-i\chi \boldsymbol{E} + \alpha_m \boldsymbol{H})(\nabla \otimes \boldsymbol{H}^*)] \\ &= \frac{1}{2}(\mathrm{Re}[\alpha_e]\mathrm{Re}[\boldsymbol{E}(\nabla \otimes \boldsymbol{E}^*) - \mathrm{Im}[\alpha_e]\mathrm{Im}[\boldsymbol{E}(\nabla \otimes \boldsymbol{E}^*) - \mathrm{Re}[\chi]\mathrm{Im}[\boldsymbol{H}(\nabla \otimes \boldsymbol{E}^*) \\ &\quad - \mathrm{Im}[\chi]\mathrm{Re}[\boldsymbol{H}(\nabla \otimes \boldsymbol{E}^*) + \mathrm{Re}[\alpha_m]\mathrm{Re}[\boldsymbol{H}(\nabla \otimes \boldsymbol{H}^*) - \mathrm{Im}[\alpha_m]\mathrm{Im}[\boldsymbol{H}(\nabla \otimes \boldsymbol{H}^*) \\ &\quad + \mathrm{Re}[\chi]\mathrm{Im}[\boldsymbol{E}(\nabla \otimes \boldsymbol{H}^*) + \mathrm{Im}[\chi]\mathrm{Re}[\boldsymbol{E}(\nabla \otimes \boldsymbol{H}^*)) \end{aligned} \tag{S3}$$

$$\begin{aligned} \mathrm{Re}[\boldsymbol{E}(\nabla \otimes \boldsymbol{E}^*)] &= \mathrm{Re}[(\boldsymbol{E} \cdot \nabla)\boldsymbol{E}^* + \boldsymbol{E} \times (\nabla \times \boldsymbol{E}^*)] \\ &= \frac{1}{2}[(\boldsymbol{E} \cdot \nabla)\boldsymbol{E}^* + [(\boldsymbol{E}^* \cdot \nabla)\boldsymbol{E} + \boldsymbol{E} \times (\nabla \times \boldsymbol{E}^*) + \boldsymbol{E}^* \times (\nabla \times \boldsymbol{E})] \\ &= \frac{1}{2}\nabla(\boldsymbol{E} \cdot \boldsymbol{E}^*) = \frac{1}{2}\nabla|\boldsymbol{E}|^2 \end{aligned} \tag{S4}$$

In the same way,

$$\mathrm{Re}[\boldsymbol{H}(\nabla \otimes \boldsymbol{H}^*)] = \frac{1}{2}\nabla|\boldsymbol{H}|^2 \tag{S5}$$

For the chiral portion,

$$
\begin{aligned}
&\mathrm{Im}[\boldsymbol{E}(\nabla \otimes \boldsymbol{H}^*) - \mathrm{Im}[\boldsymbol{H}(\nabla \otimes \boldsymbol{E}^*) \\
&= \mathrm{Im}[(\boldsymbol{E}\cdot\nabla)\boldsymbol{H}^* + \boldsymbol{E}\times(\nabla\times\boldsymbol{H}^*) - (\boldsymbol{H}\cdot\nabla)\boldsymbol{E}^* \text{-} \boldsymbol{H}\times(\nabla\times\boldsymbol{E}^*)] \\
&= \mathrm{Im}[(\boldsymbol{E}\cdot\nabla)\boldsymbol{H}^* + \boldsymbol{E}\times(\nabla\times\boldsymbol{H}^*) + (\boldsymbol{H}^*\cdot\nabla)\boldsymbol{E} + \boldsymbol{H}^*\times(\nabla\times\boldsymbol{E})] \\
&= \nabla\,\mathrm{Im}[\boldsymbol{E}\cdot\boldsymbol{H}^*]
\end{aligned} \tag{S6}
$$

$$
\begin{aligned}
&\mathrm{Re}[\boldsymbol{E}(\nabla \otimes \boldsymbol{H}^*) - \mathrm{Re}[\boldsymbol{H}(\nabla \otimes \boldsymbol{E}^*)] \\
&= \mathrm{Re}[(\boldsymbol{E}\cdot\nabla)\boldsymbol{H}^* + \mathrm{E}\times(\nabla\times\boldsymbol{H}^*) + (\boldsymbol{H}^*\cdot\nabla)\boldsymbol{E} + \boldsymbol{H}^*\times(\nabla\times\boldsymbol{E})] \\
&= 4\omega^2\boldsymbol{S} - 2c^2\nabla\times\bar{\boldsymbol{P}}
\end{aligned} \tag{S7}
$$

where

$$
\bar{\boldsymbol{P}} = \frac{\mathrm{Re}[\boldsymbol{E}\times\boldsymbol{H}^*]}{2c^2},\ \boldsymbol{S} = \boldsymbol{S_e} + \boldsymbol{S_m},\ \boldsymbol{S_e} = -\frac{\varepsilon_0}{\mu_b}\frac{1}{4\omega i}\boldsymbol{E}\times\boldsymbol{E}^*, \boldsymbol{S_m} = -\frac{\mu_0}{\varepsilon_b}\frac{1}{4\omega i}\boldsymbol{H}\times\boldsymbol{H}^*
$$

Thus, S3 can be written as:

$$
\begin{aligned}
\langle \boldsymbol{F}_{EM} \rangle = &\frac{\mathrm{Re}[\alpha_e]}{\varepsilon_0\varepsilon_b}\nabla\bar{W}_e + \frac{\mathrm{Re}[\alpha_m]}{\mu_0\mu_b}\nabla\bar{W}_m + \frac{2\omega\mu_b}{\varepsilon_0}\mathrm{Im}[\alpha_e]\bar{\boldsymbol{P}}_{\boldsymbol{e}}^{\boldsymbol{o}} + \frac{2\omega\varepsilon_b}{\mu_0}\mathrm{Im}[\alpha_m]\bar{\boldsymbol{P}}_{\boldsymbol{m}}^{\boldsymbol{o}} \\
&+ c\,\mathrm{Re}[\chi]\nabla\bar{K} + \mathrm{Im}[\chi](2\omega^2\boldsymbol{S} - c^2\nabla\times\bar{\boldsymbol{P}})
\end{aligned} \tag{S8}
$$

where $\bar{W}_e = \frac{1}{4}\varepsilon_0\varepsilon_b|\boldsymbol{E}|^2$, $\bar{W}_m = \frac{1}{4}\mu_0\mu_b|\boldsymbol{H}|^2$, $\bar{K} = \frac{1}{2c}\mathrm{Im}[\boldsymbol{E}\cdot\boldsymbol{H}^*]$

$$
\bar{\boldsymbol{P}}_{\boldsymbol{e}}^{\boldsymbol{o}} = -\frac{\varepsilon_0}{4\omega\mu_b}\mathrm{Im}[\boldsymbol{E}(\nabla\otimes\boldsymbol{E}^*)],\ \bar{\boldsymbol{P}}_{\boldsymbol{m}}^{\boldsymbol{o}} = -\frac{\mu_0}{4\omega\varepsilon_b}\mathrm{Im}[\boldsymbol{H}(\nabla\otimes\boldsymbol{H}^*)]
$$

The last terms in (S2) can be written as:

$$
\begin{aligned}
\langle \boldsymbol{F}_{INT} \rangle &= -\frac{ck^4}{12\pi}\mathrm{Re}[(\boldsymbol{p}\times\boldsymbol{m}^*)] \\
&= -\frac{ck^4}{12\pi}\mathrm{Re}[(\alpha_e\boldsymbol{E} + i\chi\boldsymbol{H})\times(i\chi^*\boldsymbol{E}^* + \alpha_m{}^*\boldsymbol{H}^*)] \\
&= -\frac{ck^4}{12\pi}((\mathrm{Re}[\alpha_e\alpha_m{}^*] + |\chi|^2)\,\mathrm{Re}[\boldsymbol{E}\times\boldsymbol{H}^*] - \mathrm{Im}[\alpha_e\alpha_m{}^*]\,\mathrm{Im}[\boldsymbol{E}\times\boldsymbol{H}^*] \\
&\quad - \mathrm{Re}[\alpha_e\chi^*](\frac{\boldsymbol{E}\times\boldsymbol{E}^*}{i})) - \mathrm{Re}[\alpha_m\chi^*](\frac{\boldsymbol{H}\times\boldsymbol{H}^*}{i}))
\end{aligned} \tag{S9}
$$

Thus,

$$\left\langle \boldsymbol{F}_{INT} \right\rangle = -\frac{c^3 k^4}{6\pi}((\mathrm{Re}[\alpha_e \alpha_m{}^*] + |\chi|^2)\bar{\boldsymbol{P}} - \frac{1}{2c^2}\mathrm{Im}[\alpha_e \alpha_m{}^*]\,\mathrm{Im}[\boldsymbol{E} \times \boldsymbol{H}^*]) \\ -\frac{c^2 k^5}{3\pi}(\frac{\mu_b}{\varepsilon_0}\mathrm{Re}[\alpha_e \chi^*]\boldsymbol{S_e} + \frac{\varepsilon_b}{\mu_0}\mathrm{Re}[\alpha_m \chi^*]\boldsymbol{S_m}) \tag{S10}$$

2. Field dynamics for the inherence field

$$W_e = \frac{1}{2}\varepsilon_0 \varepsilon_b A^2 (1 + \mathrm{M} \cdot \mathrm{Re}[(\cos 2\theta + \mathrm{m_1 m_2^*}) e^{i\varphi}])$$

$$W_m = \frac{1}{2}\varepsilon_0 \varepsilon_b A^2 (1 + \mathrm{M} \cdot \mathrm{Re}[(\mathrm{m_1 m_2^*} \cos 2\theta + 1) e^{i\varphi}])$$

$$\bar{\boldsymbol{P}}_{\boldsymbol{e}}^{\boldsymbol{o}} = \frac{\cos\theta}{c n_b} w_e \ \hat{\mathrm{z}} \qquad\qquad \bar{\boldsymbol{P}}_{\boldsymbol{m}}^{\boldsymbol{o}} = \frac{\cos\theta}{c n_b} w_m \ \hat{\mathrm{z}}$$

$$\bar{K} = \frac{1}{2}\frac{\varepsilon_0 \varepsilon_b}{n_b} A^2 (\sigma_1 + \sigma_2 + 2\mathrm{M}\cos^2\theta \ \mathrm{Im}[(\mathrm{m_1} - \mathrm{m_2^*}) e^{i\varphi}])$$

$$2\omega^2 \boldsymbol{S} - c^2 \nabla \times \bar{\boldsymbol{P}} = \varepsilon_0 \sqrt{\frac{\varepsilon_b}{\mu_b}} A^2 \omega \begin{Bmatrix} \sin\theta(\sigma_1 - \sigma_2)\hat{\mathrm{x}} \\ \cos\theta(\sigma_1 + \sigma_2 + 2\mathrm{M}\cos^2\theta \mathrm{Im}[(\mathrm{m_1} - \mathrm{m_2^*}) e^{i\varphi}])\hat{\mathrm{z}} \end{Bmatrix} \tag{S11}$$

$$\bar{\boldsymbol{P}} = \frac{1}{2}\sqrt{\frac{\varepsilon_0 \varepsilon_b}{\mu_0 \mu_b}}\frac{A^2}{c^2} \begin{Bmatrix} -\mathrm{M}\sin 2\theta \mathrm{Re}[(\mathrm{m_1} - \mathrm{m_2^*}) e^{i\varphi}]\hat{\mathrm{y}} \\ \cos\theta(2 + 2\mathrm{M}\mathrm{Re}[(1 + \mathrm{m_1 m_2^*}) e^{i\varphi}])\hat{\mathrm{z}} \end{Bmatrix}$$

$$\mathrm{Im}[\boldsymbol{E} \times \boldsymbol{H}^*] = \sqrt{\frac{\varepsilon_0 \varepsilon_b}{\mu_0 \mu_b}} A^2 \begin{Bmatrix} 2\,\mathrm{M}\sin\theta \mathrm{Im}[(1 - \mathrm{m_1 m_2^*}) e^{i\varphi}]\hat{\mathrm{x}} \\ \mathrm{M}\sin 2\theta \mathrm{Im}[(\mathrm{m_1} + \mathrm{m_2^*}) e^{i\varphi}]\hat{\mathrm{y}} \end{Bmatrix}$$

$$\boldsymbol{S_e} = \frac{1}{4\omega}\frac{\varepsilon_0}{\mu_b} A^2 \begin{Bmatrix} \sin\theta(\sigma_1 - \sigma_2 - 2\mathrm{M} \cdot \mathrm{Im}[(\mathrm{m_1} + \mathrm{m_2^*}) e^{i\varphi}])\hat{\mathrm{x}} \\ 2\mathrm{M} \cdot \sin 2\theta \mathrm{Im}[e^{i\varphi}]\hat{\mathrm{y}} \\ \cos\theta(\sigma_1 + \sigma_2 + 2\mathrm{M} \cdot \mathrm{Im}[(\mathrm{m_1} - \mathrm{m_2^*}) e^{i\varphi}])\hat{\mathrm{z}} \end{Bmatrix}$$

$$\boldsymbol{S_m} = \frac{1}{4\omega}\frac{\varepsilon_0}{\mu_b} A^2 \begin{Bmatrix} \sin\theta(\sigma_1 - \sigma_2 + 2\mathrm{M} \cdot \mathrm{Im}[(\mathrm{m_1} + \mathrm{m_2^*}) e^{i\varphi}])\hat{\mathrm{x}} \\ 2\mathrm{M} \cdot \sin 2\theta \mathrm{Im}[\mathrm{m_1 m_2^*} e^{i\varphi}]\hat{\mathrm{y}} \\ \cos\theta(\sigma_1 + \sigma_2 + 2\mathrm{M} \cdot \mathrm{Im}[(\mathrm{m_1} - \mathrm{m_2^*}) e^{i\varphi}])\hat{\mathrm{z}} \end{Bmatrix} \tag{S12}$$

Coefficient $M = \dfrac{1}{\sqrt{1 + |m_1|^2}\sqrt{1 + |m_2|^2}}$, $\varphi = 2kx\sin\theta$ is the relative phase difference,

and helicities $\sigma_{1,2} = \dfrac{2\,\mathrm{Im}[m_{1,2}]}{1 + |m_{1,2}|^2}$

The Stoke parameters *T, X* and *Σ* can also be represented by $\mathrm{m_1}$ and $\mathrm{m_2}$ as

$$T_{1,2} = \frac{1-\left|m_{1,2}\right|^2}{1+\left|m_{1,2}\right|^2} \qquad X_{1,2} = \frac{2\,\mathrm{Re}[m_{1,2}]}{1+\left|m_{1,2}\right|^2} \qquad \Sigma_{1,2} = \frac{2\,\mathrm{Im}[m_{1,2}]}{1+\left|m_{1,2}\right|^2}$$

3. Derivation of scattering coefficients of chiral particles

The scattering coefficient of a spherical chiral particle is defined as following.[1]

$$a_n = \frac{V_n^L A_n^R + V_n^R A_n^L}{V_n^L W_n^R + V_n^R W_n^L},$$

$$b_n = \frac{B_n^L W_n^R + B_n^R W_n^L}{V_n^L W_n^R + V_n^R W_n^L},$$

$$c_n = i\frac{A_n^L W_n^R - A_n^R W_n^L}{V_n^L W_n^R + V_n^R W_n^L}$$

when j=L,R

$$W_n^{(j)} = F\psi_n(ak_j)\xi'_n(ak_m) - \psi_n'(ak_j)\xi_n(ak_m),$$

$$V_n^{(j)} = \psi_n(ak_j)\xi'_n(ak_m) - F\psi_n'(ak_j)\xi_n(ak_m),$$

$$A_n^{(j)} = F\psi_n(ak_j)\psi'_n(ak_m) - \psi_n'(ak_j)\psi_n(ak_m),$$

$$B_n^{(j)} = \psi_n(ak_j)\psi'_n(ak_m) - F\psi_n'(ak_j)\psi_n(ak_m),$$

where $F = \sqrt{\varepsilon_r\mu_b / (\varepsilon_b\mu_r)}$. ε_r , μ_r and ε_b , μ_b are the permittivity and permeability of the particle and background respectively. $\psi_n(x) = xj_n(x)$ and $\xi_n(x) = xh_n^1(x)$ when $j_n(x)$ and $h_n^1(x)$ are the spherical Bessel function and spherical Hankel function of the first kind. $k_m = k_0\sqrt{\varepsilon_p\mu_p}$, $k_L = k_0(\sqrt{\varepsilon_p\mu_p} + \kappa)$, $k_R = k_0(\sqrt{\varepsilon_p\mu_p} - \kappa)$ are the wave numbers for mean, left-handed and right-handed polarizations in a chiral medium.

By solving the far-field scattering electric field for a chiral dipole (n=1)[2], the polarizabilities could be derived as following.

$$a_e = \frac{i6\pi\varepsilon_b\varepsilon_0}{k_b^{\,3}} a_1,\ a_m = \frac{i6\pi\mu_b\mu_0}{k_b^{\,3}} b_1,\ \chi = \frac{6\pi\sqrt{\varepsilon_b\mu_b}}{\mathrm{c}\,k_b^{\,3}} c_1$$

where $k_b = k_0\sqrt{\varepsilon_b\mu_b}$.

4. Trapping forces and lateral forces under different polarization states

The trapping forces and lateral forces under different polarization states are plotted in this section to illustrate how the polarization states play a sophisticated role in separating chiral objects in the interference field.

4.1 S/P-polarized light generates zero lateral forces on chiral at the trapping positons. When $m_1 = m_2 = 0$ (Case A in main text):

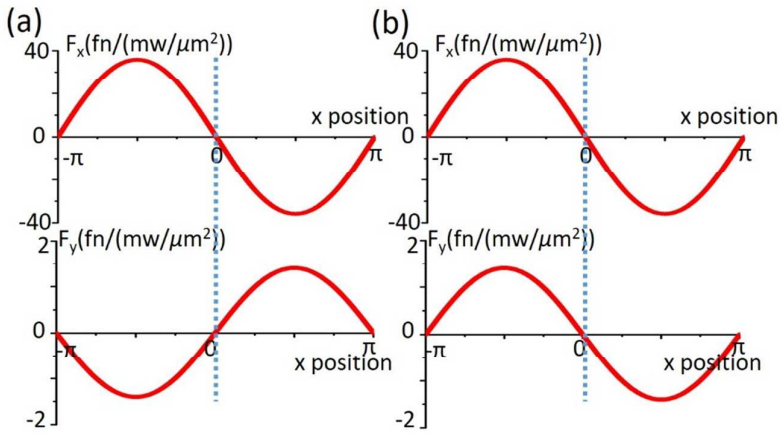

Figure S1. Trapping force F_x and lateral force F_y in the field with polarization characterized by $m_1 = m_2 = 0$ for chiral particles with (a) κ= -0.1 and (b) κ=0.1. SiO_2 particle with size of ka=1 are considered.

4.2 When both waves are linear polarized but not completely horizontal or vertical, non-zero lateral forces are gained at the particles' trapping positions. However, the lateral forces are in the same direction for chiral particles with opposite handedness. When the polarization states are mirror symmetric m_1=1and m_2=-1(Case B in main text):

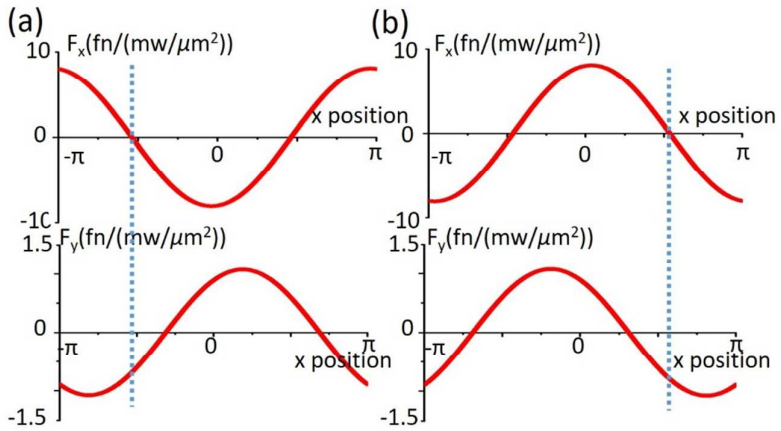

Figure S2. Trapping force F_x and lateral force F_y in the field with polarization characterized by m_1=1 and m_2=-1 for chiral particles with (a) κ= -0.1 and (b) κ=0.1 SiO_2 particle with size of ka=1 are considered.

When the polarization states are not mirror symmetric but two arbitrary chosen angles 75 degree and 30 degree with m_1=tan(75) and m_2= -tan(30):

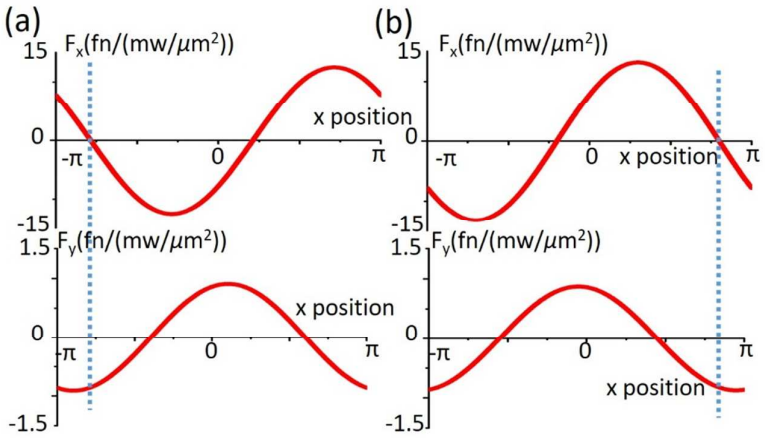

Figure S3. Trapping force F_x and lateral force F_y in the field with polarization characterized by m_1=tan(75) and m_2= -tan(30) for chiral particles with (a) κ= -0.1 and (b) κ=0.1 SiO_2 particle with size of ka=1 are considered.

4.3 When both waves are circular polarized with opposite handedness, the forces are similar to case 4.2. When both waves are circular polarized with same handedness, the forces are similar to case 4.1 (not plotted here). When the polarization states are circular polarized with opposite handedness m_1=i and m_2=-i:

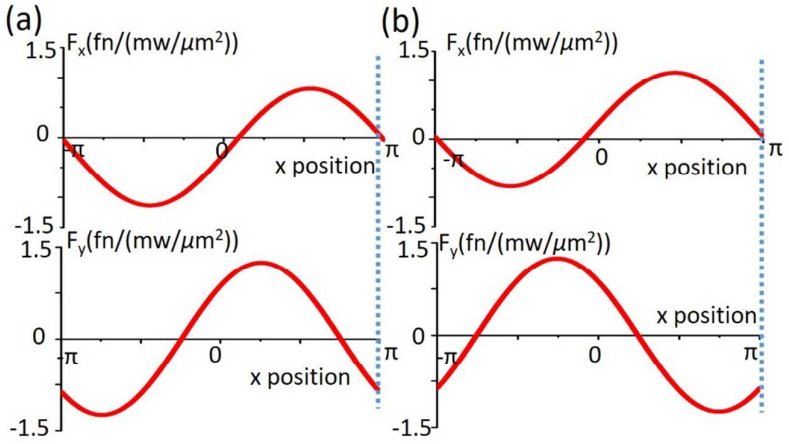

Figure S4. Trapping force F_x and lateral force F_y in the field with polarization characterized by m_1=i and m_2= -i for chiral particles with (a) κ= -0.02 and (b) κ=0.02 SiO_2 particle with size of ka=1 are considered.

4.4 When one wave is linear polarized and the other wave is circular polarized, non-zero lateral forces are gained at the particles' trapping positions. The lateral forces are in the opposite direction for chiral particles with opposite handedness. The separation could be achieved. When the polarization states are one linear and the other circular m_1=1and m_2=i:

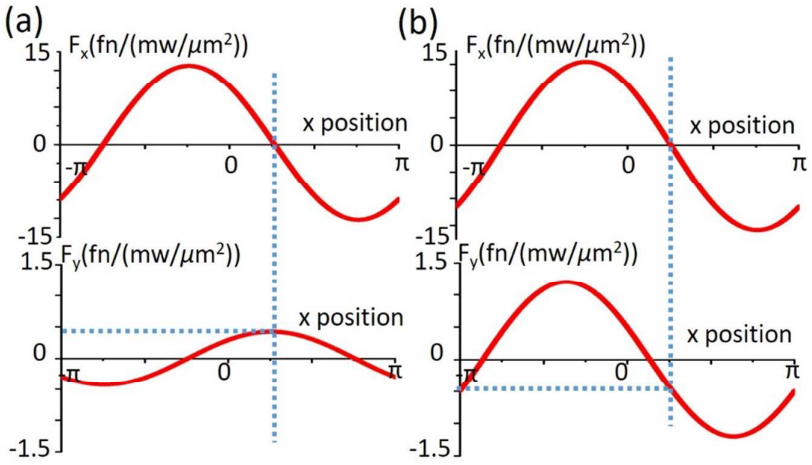

Figure S5. Trapping force F_x and lateral force F_y in the field with polarization characterized by m_1=1 and m_2= i for chiral particles with (a) κ= -0.1 and (b) κ=0.1 SiO_2 particle with size of ka=1 are considered.

5. Optical sorting of chiral particles with size beyond dipole region at the interface of air and water

The chirality-sensitive lateral force at the interface of air and water is robust for particles with sizes in a wide range. As plotted in the figure S6, chirality sorting on particles with size of ka=2, 3 and 5 could be implemented.

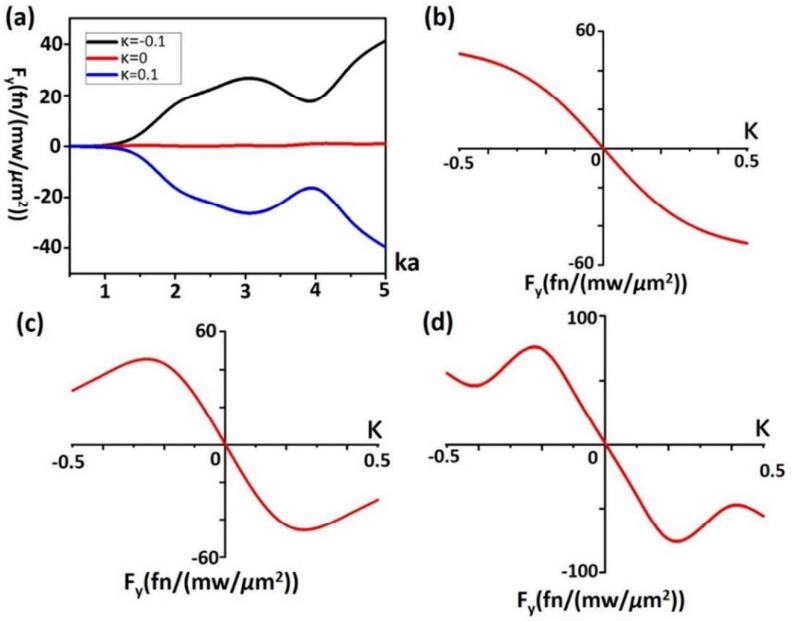

Figure S6. (a) Lateral forces when particles are at the interface of air and water at varying size. At varying chirality parameter κ on particles with size of (b) ka=2, (c) ka=3 and (d) ka=5. Wavelength of 532nm light in s-polarization is incident at the angle of 45 degree at the interface of air and water.

The following figure show the lateral force on 1μm chiral particle at the interface of air and water.

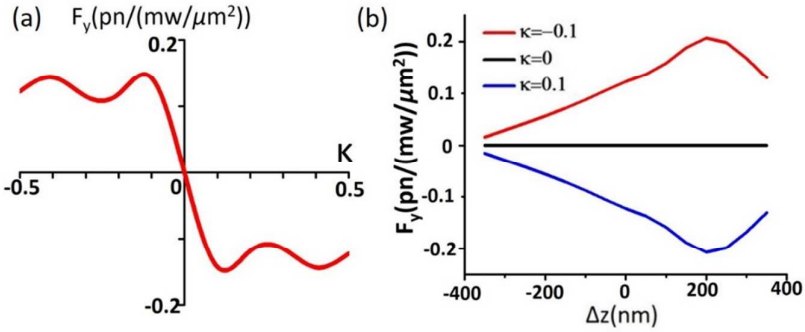

Figure S7. (a) Lateral force on SiO_2 chiral particle with size of 1μm in diameter at the interface of air and water. 532nm wavelength light in p-polarization is incident at the angle of 45 degree at the interface of air and water. (b) Lateral force acting on the chiral particle when varying its vertical position z.

6. Optical sorting of chiral particles with other shapes

Chirality-sensitive lateral forces are also found on objects with different shapes. We calculated the lateral force on cylindrical object with length of 300nm and radius of 80nm and ellipse object with major radius of 150nm and two minor radius of 80nm for two beams configuration case D and the interface case when their long axis are along different directions.

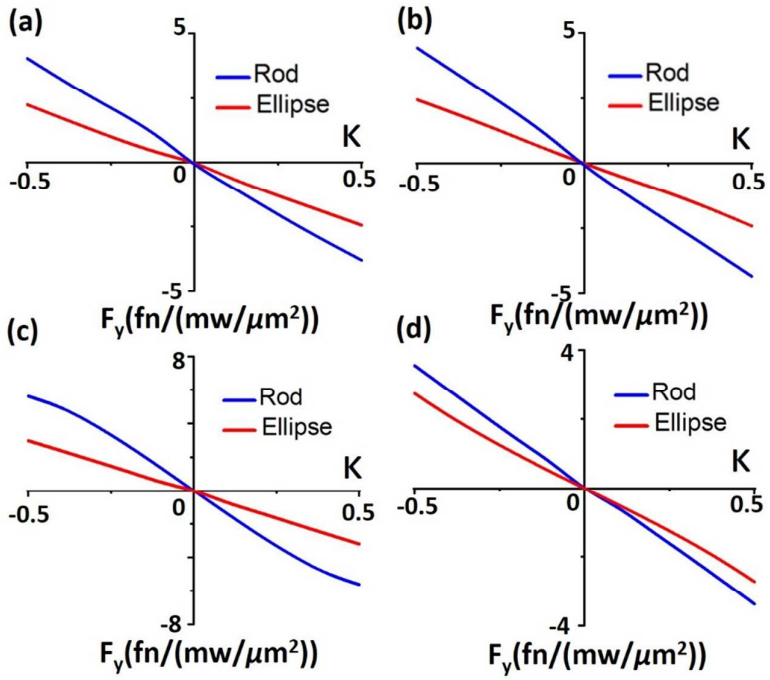

Figure S8. Lateral forces on rod and ellipse objects for case D and the interface case. Case D: lateral force when varying chirality parameter κ when their long axis are along the longitudinal direction (a) and lateral direction (b). The interface case: lateral force when varying chirality parameter κ when their long axis are along the longitudinal direction (c) and lateral direction (d).

7. Stable manipulation at the interface by lateral force

Manipulations of micrometer scale particles at the interface of air and water have already been demonstrated in experiments[3,4] and manipulation of particle sub-wavelength size is also practical. In vertical direction (z direction), following a previous paper[5] (section 5 of supplementary materials), for a particle with radius of 100nm, the unit of surface energy is $\sigma_{w/a} = 2.26\text{x}10^{-15}$J, which is much larger than the thermal energy $k_BT \sim 4.1\text{x}10^{-21}$J , the gravity energy of $4/3\pi r^3 \cdot \rho g r$ in order of 10^{-24}J and radiation pressure in vertical direction in order of 10^{-21}J. Therefore,

the surface energy well can trap the particle stably at the interface from the Brownian motion. To float the particle at the interface easier, water with salts or liquid with higher density could be used since our sorting method is applicable to an interface between any two different media. Once the chiral particle is trapped at the interface in vertical direction, the optical field will exert continuous lateral force on it despite of particle's vertical and horizontal positions as shown in Figure. 5b. In the horizontal plane (x-y plain), the lateral forces will push the particles continuously to the sides of the beam despite of the presence of Brownian motion. We calculated the trajectories of chiral particles in radius of 100nm and 500nm with opposite handedness using Langevin equation plotted in the following figure. It is obvious that the chiral particles could overcome the Brownian motion and move to the sides under the lateral force. Two flows could be added to the side of the beam to collect the chiral particles. The radiation pressure in the longitudinal direction (x direction) could be prevented by using optical line trap as done in the previous experiment.[4]

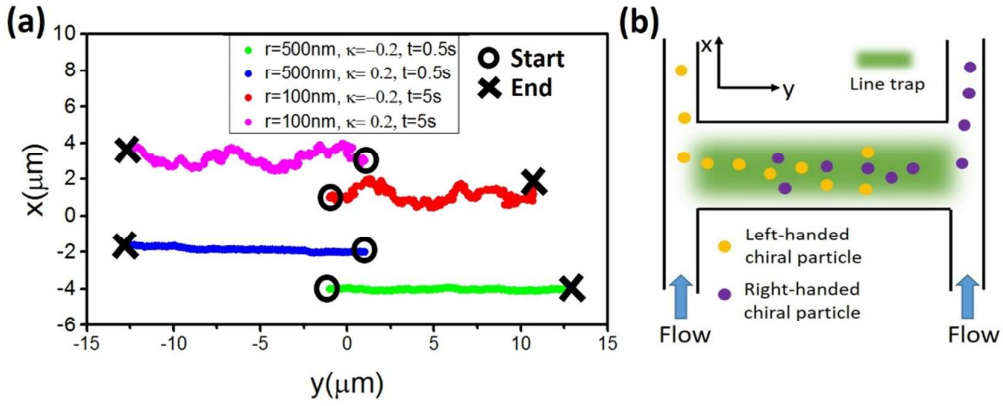

Figure S9. (a) Calculated trajectories on 100nm and 500nm chiral particles with opposite handedness by Langevin equation. Supposing the chiral particles have the same density and refractive index with PS particles which are used in previous experiment[4] and the radiation pressures in longitudinal direction (x direction) are eliminated by optical line trap.[4] Temperature is 298°and incident power is 1mw/μm^2. The drag coefficient is set to half of that in Stokes formula which is verified in previous experiment.[4] (b) Proposed schematic for sorting chiral particles at the interface using optical line trap in a flow chamber.

Supplementary Reference

1. Bohren, C. F.; Huffman, D. R., *Absorption and Scattering of Light by Small Particles*. John Wiley & Sons: 2008.

2. Wang, S. B.; Chan, C. T., Lateral Optical Force on Chiral Particles near a Surface. *Nat. Commun.* **2014,** *5*, 3307.

3. Kajorndejnukul, V.; Ding, W. Q.; Sukhov, S.; Qiu, C. W.; Dogariu, A., Linear Momentum Increase and Negative Optical Forces at Dielectric Interface. *Nat. Photonics* **2013,** *7*, 787-790.

4. Sukhov, S.; Kajorndejnukul, V.; Naraghi, R. R.; Dogariu, A., Dynamic Consequences of Optical Spin-Orbit Interaction. *Nat. Photonics* **2015,** *9*, 809-812.

5. Qiu, C.-W.; Ding, W.; Mahdy, M.; Gao, D.; Zhang, T.; Cheong, F. C.; Dogariu, A.; Wang, Z.; Lim, C. T., Photon Momentum Transfer in Inhomogeneous Dielectric Mixtures and Induced Tractor Beams. *Light: Science & Applications* **2015,** *4*, e278.